

## Twin boundaries: Strong or weak?

S. Qu, P. Zhang, S.D. Wu, Q.S. Zang and Z.F. Zhang\*

*Shenyang National Laboratory for Materials Science, Institute of Metal Research, Chinese Academy of Sciences,  
WenHua Road 72, Shenyang, 110016, PR China*

Received 31 March 2008; revised 9 July 2008; accepted 25 July 2008  
Available online 3 August 2008

Fatigue cracking along twin boundaries (TBs) has significantly different features in Cu and Cu–Al alloys. In Cu and Cu–5 at.% Al alloy, the TBs are intrinsically strong and resist fatigue cracking. With the decrease in stacking fault energy (SFE), some fatigue cracks were observed along or near the TBs in Cu–16 at.% Al alloys. The current findings confirm that the TBs are not always strong enough to prevent fatigue cracking, which is also affected by SFE or slip mode.

© 2008 Published by Elsevier Ltd. on behalf of Acta Materialia Inc.

*Keywords:* Cu–Al alloy; Twin boundary; Fatigue cracking; Stacking fault energy

Study of the fatigue damage mechanisms of metallic materials is essential for theoretical understanding and engineering applications. Since the 1950s, it has been gradually recognized that fatigue cracking along persistent slip bands (PSBs) is one of the important damage mechanisms in both single-crystal and polycrystalline materials [1,2]. From the 1970s to 1990s, a number of researchers devoted much effort to investigating the fatigue damage associated with the PSBs during cyclic deformation of Cu crystals. For example, Finney and Laird [3], Basinski and Basinski [4] and Essmann et al. [5] systematically revealed the fatigue cracking mechanisms associated with the intrusion and extrusion of PSBs. In addition, some other reports showed that grain boundaries (GBs) often become the preferential sites for the induction of fatigue cracks mainly in polycrystalline materials. Kim and Laird [6] proposed a step mechanism for fatigue cracking along GBs at high strain amplitude in polycrystalline Cu. Mughrabi et al. [7,8] proposed another mechanism based on the interactions between PSBs and GBs in polycrystalline Cu by taking account of piling-up of dislocations at GBs due to irreversible slip during cyclic deformation. Recently, Zhang et al. [9–11] employed a series of Cu bicrystals to reveal the fatigue cracking mechanisms along different large-angle GBs, and found that those large-angle GBs always become the preferential sites for fatigue cracking. This gives rise to an interesting question: what kinds of

GBs are intrinsically strong enough to resist fatigue cracking?

In addition to the common large-angle GBs, there is another special GB, i.e. twin boundary (TB), alongside which atoms often have very good coherent relationship. Interestingly, the TBs were found to significantly improve the strength and plasticity of some nanostructured Cu with a high density of nanoscale twins [12]. However, in comparison with common large-angle GBs, there is no experimental evidence to determine whether TBs are strong enough to resist fatigue cracking. There are several classical reports about the fatigue cracking mechanisms beside TBs. Thompson et al. [13] proposed that local enhancement of plastic strain in planes parallel to TBs might be due to both elastic anisotropy and changes in the dislocation structure in regions close to the twins; this finding was later confirmed by Bottner et al. [14]. Hook and Hirth [15] first showed that elastic interaction stress developed at a Fe–Si bicrystal boundary, resulting from the mismatch of the elastic constants, which was associated with TB-cracking. Later, Nenmann et al. [16] and Heinz et al. [17] carried out calculations to rationalize the observation that fatigue cracking would take place at every other boundary in a stack of twins of Cu and austenitic steel. Their calculations were consistent with the observations that cracking occurred at those TB sites with the highest stress. Gopalan and Margolin [18] found evidence that slip produced due to compatibility of the TBs assisted the formation of fatigue cracking. In 1994, Peralta et al. [19] proposed a model to account for both

\* Corresponding author. Tel.: +86 24 23971043; fax: +86 24 2389 1320; e-mail: [zhfzhang@imr.ac.cn](mailto:zhfzhang@imr.ac.cn)

the compatibility of TBs and the effect of the orientation of the tensile axis on fatigue cracking. Based on the above literature, research has mainly ascribed TB-cracking to the elastic stresses arising from the elastic anisotropy and the changes in the dislocation structure in the vicinity of TBs. However, it is not very clear how the intrinsic parameters, such as stacking fault energy (SFE) and slip mode, affect the fatigue cracking behavior of TBs. It is well known that cold-rolled polycrystalline Cu and Cu–Al alloys can form many annealing twins after annealing at high temperature. In the current research, we will systematically reveal whether the TBs in polycrystalline Cu and Cu–Al alloys with different Al contents are strong enough to resist fatigue cracking or not. Based on the experimental results, the differences in the fatigue cracking behaviors along the TBs are further discussed.

The materials used in this study are commercially pure Cu and three Cu–Al alloys with different Al contents (Cu–5 at.% Al, Cu–8 at.% Al and Cu–16 at.% Al). The SFE of the Cu–Al alloys gradually decreases from about  $40 \text{ mJ m}^{-2}$  for pure Cu to  $2.5 \text{ mJ m}^{-2}$  for Cu–16 at.% Al [20]. The three Cu–Al alloys were prepared from high-purity (99.999%) Cu by vacuum casting and forged into plates at  $800 \text{ }^\circ\text{C}$ . The fatigue specimens were spark machined from the annealed plates to have a gauge dimension of  $16 \times 5 \times 4 \text{ mm}$ . Before fatigue testing, the specimens were annealed at  $800 \text{ }^\circ\text{C}$  for 2 h in an Ar atmosphere. A large number of annealing twins were formed in pure Cu and  $\alpha$ Cu–Al alloys and the fraction of the annealing twins increased with increasing Al content. Symmetrical pull–push cyclic deformation tests were performed at room temperature on a Shimadzu fatigue testing machine under constant plastic strain amplitude control in the range of  $1 \times 10^{-4}$  to  $4 \times 10^{-3}$ . After cyclic deformation, the surface deformation morphologies of pure Cu and Cu–Al alloy specimens were carefully observed by scanning electron microscope (SEM) to reveal the slip morphologies and evolution of fatigue cracks at different strain amplitudes.

Figure 1 shows the typical slip morphologies near the annealing TBs in pure Cu and Cu–Al alloys with different Al contents cyclically deformed at different strain amplitudes. It can be seen that many slip bands (SBs) appear in the pure Cu specimen and the SBs are often very coarse and scraggy, exhibiting obvious extrusions or intrusions, as shown in Figure 1a. However, the SBs in Cu–5 at.% Al specimen become slightly finer than those of pure Cu, but were still a persistent feature. The plastic strain localization also occurs within the SBs in Cu–5 at.% Al alloy, as that in pure Cu, and the severely deformed SBs can transfer through the TBs (see Fig. 1b). The deformation morphology of Cu–8 at.% Al alloy displays a planar slip feature and its SBs are smooth and straight, as shown in Figure 1c. It can be seen that the densities of the SBs are different at both sides of TBs and the severely deformed SBs cannot always transfer through the TBs (see Fig. 1c). The Cu–16 at.% Al alloy exhibits typical planar slip features, and the SBs are very fine and homogeneously distributed on the deformation surface. The density of the SBs is highest among these Cu–Al alloys and the SBs are interlaced and distributed

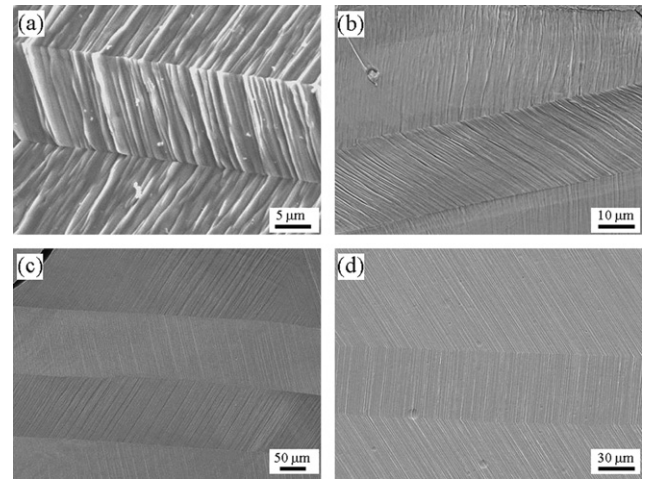


**Figure 1.** Surface slip morphologies along TBs in fatigued polycrystalline material: (a) pure Cu at a strain amplitude of  $1.0 \times 10^{-3}$  for 5000 cycles; (b) Cu–5 at.% Al alloy at a strain amplitude of  $3.0 \times 10^{-3}$  for 5000 cycles; (c) Cu–8 at.% Al alloy at a strain amplitude of  $3.5 \times 10^{-3}$  for 5000 cycles; and (d) Cu–16 at.% Al alloy at a strain amplitude of  $3.0 \times 10^{-3}$  for 5000 cycles.

along TBs (see Fig. 1d). Consequently, it can be concluded that with the decrease in the SFE of Cu–Al alloys, the nature of slip mode has changed from a wavy slip to a planar slip during fatigue. The deformation of pure Cu and Cu–5 at.% Al alloy is intensely localized in SBs, and these severely deformed SBs are symmetrically distributed along TBs. Therefore, the SBs can transfer through the TBs continuously. However, for Cu–8 at.% Al and Cu–16 at.% Al alloys, their slip morphologies become more homogeneous and the densities of the SBs besides the TBs are different, sometimes leading to a discontinuity of the adjacent SBs across the TBs.

The fatigue cracking observations show that the common large-angle GBs often become the preferential sites for the initiation of fatigue cracks for both pure Cu and Cu–Al alloys. However, there are two different modes for fatigue cracking near the TBs with the decrease in the SFE of the Cu–Al alloys. In pure Cu and Cu–5 at.% Al alloy, due to the strong plastic strain location within the SBs, fatigue cracks were found to nucleate along those severely plastic deformed SBs, which is consistent with the results in single-crystal and polycrystalline Cu [5,13]. Moreover, these fatigue cracks along SBs have a good one-to-one relationship across the TBs into the neighboring twin grains, as shown in Figure 2a and b. We can define this cracking mode as slip band crack, i.e. SB-crack. However, the fatigue cracking along the TBs in pure Cu and Cu–5 at.% Al alloy was not observed. As a transition from the wavy slip mode to planar slip mode, there are two SB-crack modes beside the TBs of Cu–8 at.% Al alloy. One fatigue cracking still nucleated along the SBs and the cracks can also transfer through the TBs, i.e. SB-crack, as shown in Figure 2c. The other fatigue cracking only localized within the SBs, but cannot transfer through the TBs. The differences in the fatigue cracking behavior along SBs should be associated with the different slip modes or SFE in Cu–Al alloys. When some SBs cannot transfer through

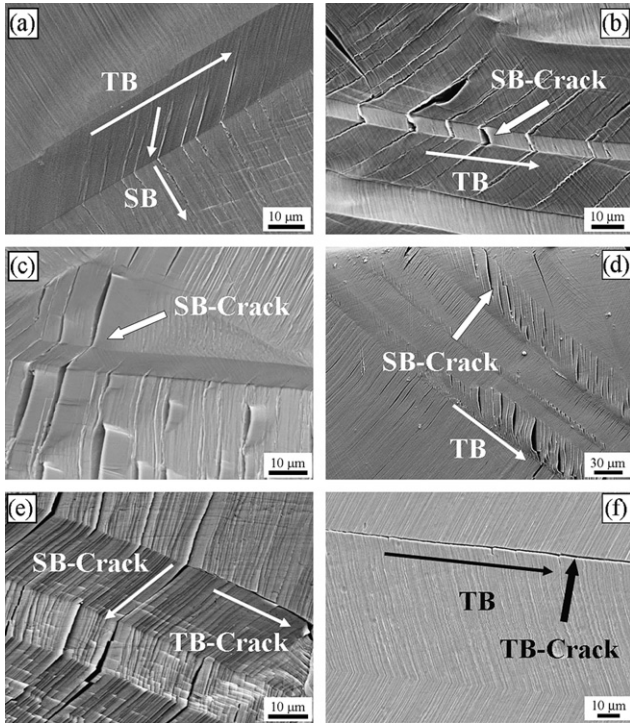


**Figure 2.** Fatigue cracking behaviors along TBs in fatigued polycrystalline Cu–Al alloy: (a) SB-cracking in Cu–5 at.% Al alloy at  $\epsilon_{pl} = 1.0 \times 10^{-3}$ ,  $N = 5000$  and (b) at  $\epsilon_{pl} = 1.0 \times 10^{-3}$ ,  $N = 10,000$ . (c)–(e) Two kinds of TB-cracks in Cu–8 at.% Al alloy at  $\epsilon_{pl} = 4.0 \times 10^{-3}$ ,  $N = 5000$ ; (f) TB-cracking in Cu–16 at.% Al alloy at  $\epsilon_{pl} = 4.0 \times 10^{-3}$ ,  $N = 5000$ .

the TBs, i.e. without the one-to-one relationship of the SBs beside the TBs, as shown in Figure 2c and d, some fatigue cracks can simultaneously occur along the SBs and the TBs, and we can define the fatigue cracking along the TBs as TB-crack, as shown in Figure 2e. Finally, for the Cu–16 at.% Al alloy, the fatigue cracks mainly nucleated along the TBs, i.e. TB-crack, as shown in Figure 2f. This indicates that the TBs are not always strong enough to resist fatigue crack, which is also affected by the SFE or slip mode in Cu–Al alloys.

It is well known that the SFE of alloys plays an important role in the slip mode [21–23]. When the SFE is high, the smaller interspatial spacing facilitates the partial dislocation pinching, consequently resulting in a greater tendency for cross-slip due to wavy dislocation substructure [24]. At higher strain levels, the dislocations in the high-SFE material tend to rearrange themselves into cell-like structures with the majority of the dislocations residing in cell walls and the interior of the cells relatively dislocation-free [22]. This leads to the large degree of the deformation locations in the PSBs on one side of TBs in the high-SFE material. Thus, under the cyclic loading conditions, the fatigue cracks easily nucleate along the severely deformed PSBs. Since the severely deformed PSBs have a one-to-one relationship on each side of the TBs, the fatigue cracks will naturally transfer through the TBs, forming the SB-crack, but TBs themselves cannot form the fatigue cracks, as shown in Figure 2a–c.

On the other hand, in the low-SFE material (Cu–16 at.% Al), dislocations tend to organize themselves into planar arrays [25,26]. The operation of this mechanism would result in both the extensive annihilation of dislocations and the formation of new planar slip bands. Initially inhomogeneous slip subsequently becomes relatively homogeneous by repeated activation of new slip bands and continual deactivation of old slip bands. Unlike with Cu, in which PSBs can carry most of the plastic deformation, the deformation of Cu–Al alloys is always localized in certain slip bands [27]. The strain location in this alloy is expected to be on a much finer scale with much shorter persistence of localization than the high-SFE pure Cu [28]. Therefore, TBs can accommodate more plastic deformation in Cu–Al alloy than in copper. As a result, the stress due to the plastic deformation in TBs of Cu–Al alloys is higher than that of copper (see Fig. 3). Moreover, under cyclic tension and compression stress, the deformation degree of the SBs adjacent to the TB is different, which makes the SBs interlace alongside the TB. For example, the SBs on one side of TB are weakly deformed; however, the SBs on another side of TB are strongly deformed, which often causes a severe strain incompatibility at the TB under cyclic loading. Therefore, the plastic strain cannot be efficiently transferred from the strong SBs to the weak SBs across the TB, as illustrated in Figure 4a and b, and some micro-scale fatigue cracks nucleated at the discontinuous points near the TB, as shown in Figure 4c and d. With the action of high stress, these discontinuous micro-scale cracks can propagate along TBs, finally leading to a TB-crack, as illustrated in Figure 4e. Therefore, TB-cracks can be more easily formed in Cu–16 at.% Al alloys than in pure Cu because of the different SFE or slip mode. In addition, it should be emphasized that more attention has been paid to the fatigue behaviors of TBs at relatively high strain amplitudes ( $>10^{-3}$ ) and low cycles ( $\leq 10,000$  cycles) in the present work. However, TBs are also important in the fracture behaviors at low stress and long lifetimes because of their stress concentration effects, and the fatigue behavior of twins under these conditions should be further

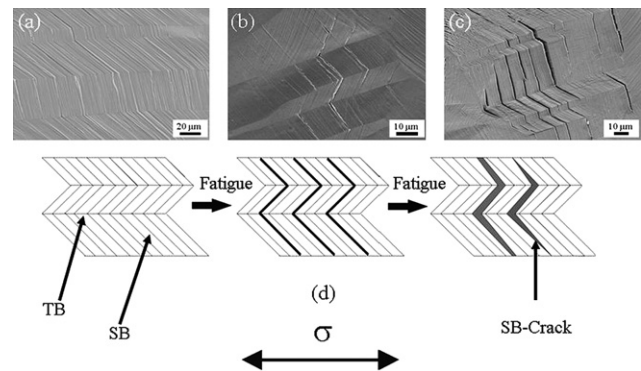


**Figure 3.** (a, b) Fatigue cracking morphologies of Cu–5 at.% Al alloy at  $\epsilon_{pl} = 1.0 \times 10^{-3}$ ,  $N = 5000$ , and (c) Cu–8 at.% Al alloy at  $\epsilon_{pl} = 4.0 \times 10^{-3}$ ,  $N = 5000$ . (d) Illustration of the SB-cracking processes in Cu–Al alloys with high-SFE.



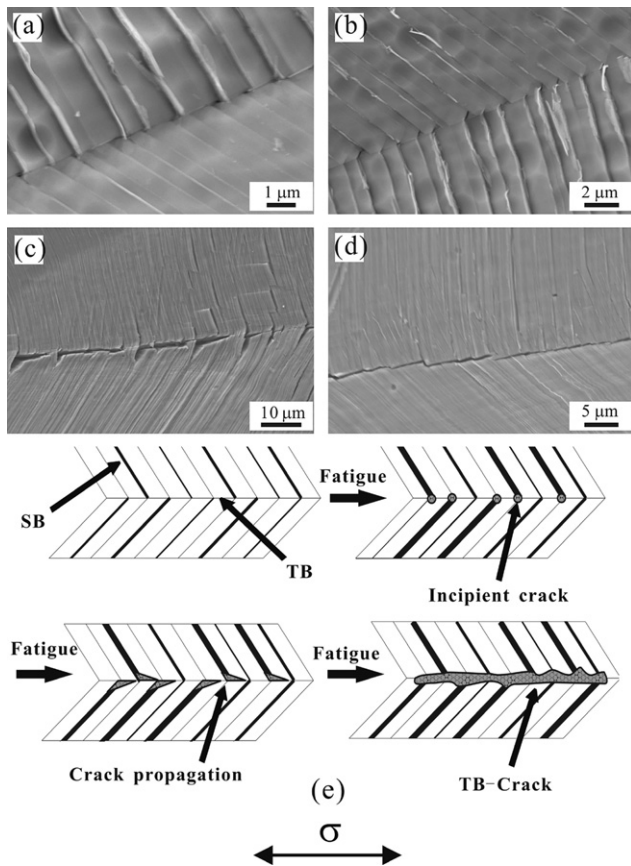


**Figure 4.** (a and b) Initial fatigue cracking morphologies, and (c and d) the final TB-cracking of Cu-16 at.% Al alloy. (e) Illustration of the TB-cracking processes in Cu-Al alloys with low-SFE.

investigated. Moreover, all the conclusions drawn in this work are based on, and can only be applied to, the conditions under which the experiments have been done.

In summary, TBs have often been considered a good interface to connect the adjacent grains in pure Cu polycrystals, which can have good tensile strength and elongation. Under cyclic loading conditions, TBs are also stronger than the common large-angle GBs in terms of resisting fatigue cracking. However, TBs in Cu-Al alloys with different Al content are not always strong enough to resist fatigue cracking. In our experiments, two kinds of cracking modes adjacent to the TBs were observed, i.e. SB and TB-cracking modes, depending on the SFE or slip mode. These new findings provide some experimental evidence for the optimum design of alloys with different SFEs to resist fatigue cracking along TBs.

This work was financially supported by the “Hundred of Talents Project” by Chinese Academy of Sciences, the National Natural Science Foundation of China (NSFC) under Grant No. 50571104, and the National Outstanding Young Scientist Foundation under Grant No. 50625103.

- [1] N. Thompson, N.J. Wadsworth, N. Louat, *Philos. Mag.* 1 (1956) 113.
- [2] P.J.E. Forsyth, *Nature* 171 (1953) 172.
- [3] J.F. Finney, C. Laird, *Philos. Mag.* 31 (1975) 339.
- [4] Z.S. Basinski, S.J. Basinski, *Acta Metall.* 37 (1989) 3263.
- [5] U. Essmann, U. Gosele, H. Mughrabi, *Philos. Mag.* A44 (1981) 405.
- [6] W.H. Kim, C. Laird, *Acta Metall.* 26 (1978) 789.
- [7] H. Mughrabi, F. Ackermann, K. Herz, *ASTM STP* 811 (1983) 5.
- [8] W. Liu, M. Bayerlein, H. Mughrabi, A. Day, P.N. Queded, *Acta Metall. Mater.* 30 (1992) 1763.
- [9] Z.F. Zhang, Z.G. Wang, S.X. Li, *Fatigue Fract. Eng. Mater. Struct.* 21 (1998) 1307.
- [10] Z.F. Zhang, Z.G. Wang, *Mater. Sci. Eng. A271* (1999) 449.
- [11] Z.F. Zhang, Z.G. Wang, *Acta Mater.* 51 (2003) 367.
- [12] L. Lu, Y.F. Shen, X.H. Chen, L.H. Qian, K. Lu, *Science* 304 (2004) 422.
- [13] N. Thompson, in: B.L. Averbach, D.K. Felbeck, J.T. Hahn, D.S. Thomas (Eds.), *Fracture, Proceedings of the International Conference on Atomic Mechanisms of Fracture*, Chapman and Hall, London, 1959, pp. 354–375.
- [14] R.C. Boettner, A.J. McEvily, Y.C. Liu, *Philos. Mag.* 10 (1964) 95.
- [15] R.E. Hook, J.P. Hirth, *Acta Metall.* 15 (1967) 535.
- [16] P. Neumann, A. Tonnessen, in: P.O. Kettunen, T.K. Lepisto, M.E. Lehtonen (Eds.), *Strength of Metals and Alloys*, Pergamon Press, Oxford, 1988, p. 743.
- [17] A. Heinz, P. Neumann, *Acta Metall. Mater.* (1990) 1933.
- [18] P. Gopalan, H. Margolin, *Mater. Sci. Eng. A142* (1992) 11.
- [19] P. Peralta, L. Llanes, J. Bassani, C. Laird, *Philos. Mag.* 70 (1994) 219.
- [20] A. Orlova, M. Pahutova, J. Cadak, *Philos. Mag.* 23 (1971) 303.
- [21] O. Johari, G. Thomas, *Acta Metall.* 12 (1964) 1153.
- [22] F.I. Grace, M.C. Inman, *Metallography* 3 (1970) 89.
- [23] C.S. Pande, P.M. Hazzledine, *Philos. Mag.* 24 (1971) 1393.
- [24] P.R. Swann, G. Thomas, J. Washburn, *The Impact of Transmission Electron Microscopy on Theories of the Strength of Crystals*, Interscience Publishers, New York, 1961.
- [25] H. Inui, S.I. Hong, C. Laird, *Acta Metall. Mater.* 38 (1990) 2261–2274.
- [26] L. Buchinger, A.S. Cheng, S. Stanzl, C. Laird, *Mater. Sci. Eng.* 80 (1986) 155.
- [27] S.I. Hong, C. Laird, *Mater. Sci. Eng. A128* (1990) 55.
- [28] B.D. Yan, A.S. Cheng, L. Buchinger, S. Stanzl, C. Laird, *Mater. Sci. Eng.* 80 (1986) 129.